Supporting Information

Superstructural Assembly of Ag_{24} Nanoclusters with Different Ligands Exhibiting Mechano-responsive Luminescence

Deepak Kumar Patel,[a] Ankit Sharma,[b,c] Arijit Jana,[a] Jayoti Roy,[a] Amoghavarsha Ramachandra Kini,[a] Vivek Yadav,[a] Subrata Duary,[a] Kumaran Nair Valsala Devi Adarsh,*[b] Sundargopal Ghosh,*[a] Thalappil Pradeep*[a]

[a]*DST Unit of Nanoscience (DST UNS) and Thematic Unit of Excellence (TUE), Department of Chemistry, IIT Madras, Chennai -600036, India.* E-mail: pradeep@iitm.ac.in, sghosh@iitm.ac.in

[b]*Department of Physics, Indian Institute of Science Education and Research Bhopal- 462066, India.* E-mail: adarsh@iiserb.ac.in

[c]*Department of Physics and Astronomy, Aarhus University, Ny Munkegade 120, DK-8000 Aarhus C Denmark*

KEYWORDS: Mechanoluminescence, Luminescence, Multi-ligands, Silver nanocluster, Aggregation-caused quenching Femtosecond spectroscopy.

Table of contents

1. Experimental Details

2. Supplementary Data

Figure S1 UV-vis absorption spectrum of Ag_{18} NC.

Figure S2 Time-dependent LEIST synthesis and size-focusing process of Ag24 monitored by UV–vis absorption spectroscopy.

Figure S3 UV-vis absorption spectra of ligand exchange between Ag_{18} and HMPP ligand

Figure S4 ^{1}H NMR of HMPP ligand in $CDCl_3$

Figure S5 ^{1}H NMR of TRZDT ligand in $CDCl_3$

Figure S6 ^{1}H NMR of Ag_{24} NC in $CDCl_3$.

Figure S7 ^{13}C NMR of Ag_{24} NC in $CDCl_3$.

Figure S8 ^{31}P NMR of Ag_{24} NC in $CDCl_3$.

Figure S9 FT-IR-spectra of TRZDT, HMPP ligands and Ag_{24} nanocluster.

Figure S10 XPS spectrum of Ag_{24} nanocluster.

Figure S11 Optical images of Ag_{24} NC aggregates and sheets..

Figure S12 FESEM images of the Ag_{24} NC sheets.

Figure S13 EDX mapping of Ag_{24} NC.

Figure S14 HR-TEM images of Ag_{24} NC.

Figure S15 PXRD of Ag_{24} nanocluster sheets.

Figure S16 UV–Vis absorption spectra of Ag_{24} NC before and after grinding.

Figure S17 The ESI mass spectrum of the ground sample.

Figure S18 Thermogravimetric analysis (TGA) of Ag_{24}.

Figure S19 Non-emissive sheets and mechanoluminescence of Ag_{24} NC.

1. Experimental Section

Materials: Silver nitrate ($AgNO_3$) was purchased from Rankem chemical. Triphenylphosphine (TPP), 2-mercapto-5-n-propylpyrimidine (HMPP), 6-(Dibutylamino)- 1,3,5-triazine-2,4-dithiol (TRZDT), and $NaBH_4$ were purchased from Sigma Aldrich. Solvent grade dichloromethane (DCM), chloroform ($CHCl_3$), n-hexane, N-N dimethylformamide (DMF), and methanol (99.5%) were purchased from Rankem chemicals and Finar, India. Milli-Q water was utilized in the synthesis of $[Ag_{18}H_{16}(TPP)_{10}]^{2+}$ NCs. Deuterated solvent CDCl3 (99.8 atom % D) was purchased from Sigma Aldrich. All chemicals were used as received without further purification.

Instrumentation and Characterization: The UV-vis spectra of nanoclusters were recorded using a Perkin Elmer Lambda 25 UV-vis spectrometer, typically measured in the range of 200-1100 nm with a 1 nm bandpass filter. A HORIBA, Jobin Yvon NanoLog fluorescence spectrometer was used for photoluminescence measurement with a 3 nm bandpass for both emission and excitation spectra. The Waters Synapt G2Si High-Definition Mass Spectrometer, which includes an electrospray source, quadrupole ion guide/trap, ion mobility cell, and TOF analyzer, was used to measure the electrospray ionization mass spectra. Nitrogen gas was used as the nebulizer gas, and all mass spectra were collected in positive ion mode under specific conditions. Nuclear magnetic resonance spectroscopy (NMR) measurements were performed at room temperature using a Bruker 500 MHz NMR spectrometer. Pure ligands (TPP, HMPP, and TRZDT) and the nanoclusters were dissolved in $CDCl_3$ to collect ^{1}H, ^{13}C, and ^{31}P NMR spectra. X-ray photoelectron spectroscopy (XPS) of alloy nanoclusters was performed using an ESCA Probe TPD spectrometer of Omicron Nanotechnology. A monochromatic Al K_α (1486.69 eV) X-ray source was used. Samples were drop-casted on a sample stub, and measurements were carried out with a constant analyzer energy of 50 eV for the survey scans and 20 eV for the specific regions. The binding energies in the spectra were calibrated with respect to the C 1s peak at 284.8 eV. Scanning electron microscopy and energy dispersive X-ray spectroscopy analysis were performed with a Verios G4 UC, FEI instrument. For TEM, samples were prepared by drop-casting the materials on a substrate (TEM grid was used for the good quality of pictures with good contrast) and drying them at room temperature. The sample was sputter coated with Au/Pd mixture to produce better-quality images without charging. Transmission electron microscopy was performed using a JEOL 3010, 300 kV instrument at an accelerating voltage of 200 kV. The accelerating voltage was kept low to reduce beam-induced damage. Samples were prepared by transferring the film on a carbon-coated copper grid and dried under ambient conditions. The excited state dynamics of samples are analyzed using ultrafast transient absorption spectroscopy. The setup consists of Spectra-Physics MaiTai oscillator, Spitfire Ti:sapphire optical amplifier to generate the 120 fs pulses centered at 800 nm. The output beams are passed through a second

harmonic β-barium borate crystal to generate the 400 nm pulses, which are used to excite the samples (pump beam). The second harmonic pulses are separated from the fundamental beam with the help of a dichroic beam splitter. Then both 400 and residual 800 nm are sent to CDP ExciPro pump-probe spectrometer. Here the pump beam passes through a chopper, and a rotating neutral density filter controls the averaging and intensity of pulses. The 800 nm pulses are sent to a computer-controlled motion controller and a rotating CaF2 crystal to produce time delayed white light continuum probe beam. Both pump and probe beam spatially overlapped on the sample, and then a change in absorbance of the probe beam was detected with the help of MS 2004 (600 lines/mm diffraction grating blazed at 600 nm) spectrometer and Si linear photodiode arrays. Then obtained data is chirp corrected to compensate for the group velocity dispersion. Elemental analysis (C, H, N, and S) of Ag_{24} was performed using a Vario EL Cube elemental analyzer and yielded C, 51.23%; H, 5.36%; N, 6.41%; and S, 7.03. Thermogravimetric analysis (TGA) was performed on a NETZSCH STA 449 F3 Jupiter instrument equipped with Proteus 6.1.0 software. Approximately 3.3 mg of sample was analyzed in an alumina crucible under nitrogen (20 mL min^{-1}) over 30-700 °C at a heating rate of 10 °C min^{-1}. Solid-state photoluminescence quantum yield (PLQY) measurements were carried out using a HORIBA Jobin Yvon FluoroMax-4 spectrofluorometer equipped with a Quanta-φ integrating sphere, with a $BaSO_4$ pellet used as the blank/reference standard.

2. Supplementary Data

Synthesis of $[Ag_{18}H_{16}(TPP)_{10}]^{2+}$ NC

Following the established protocols[1], Ag_{18} NC was synthesized by dissolving 20mg of $AgNO_3$ in 5 mL of methanol at room temperature. Next, 70 mg of TPP was dissolved in 9 mL of $CHCl_3$ and added to the reaction mixture while stirring. After 20 minutes, 6.5 mg $NaBH_4$ dissolved in 0.75 mL milli-Q water was added to the reaction. The reaction mixture transitioned from yellow to dark brownish and finally to dark green after 3.5 hours, indicating the formation of Ag_{18} NC. After completion, mixed solvents were removed under reduced pressure. Excess salts were eliminated by dissolving the dark greenish NC in cold water and extracting it with methanol to obtain purified Ag_{18} NC. Mass spectrometric results and UV-vis absorption spectra confirmed the formation of the NC (Figure S1).

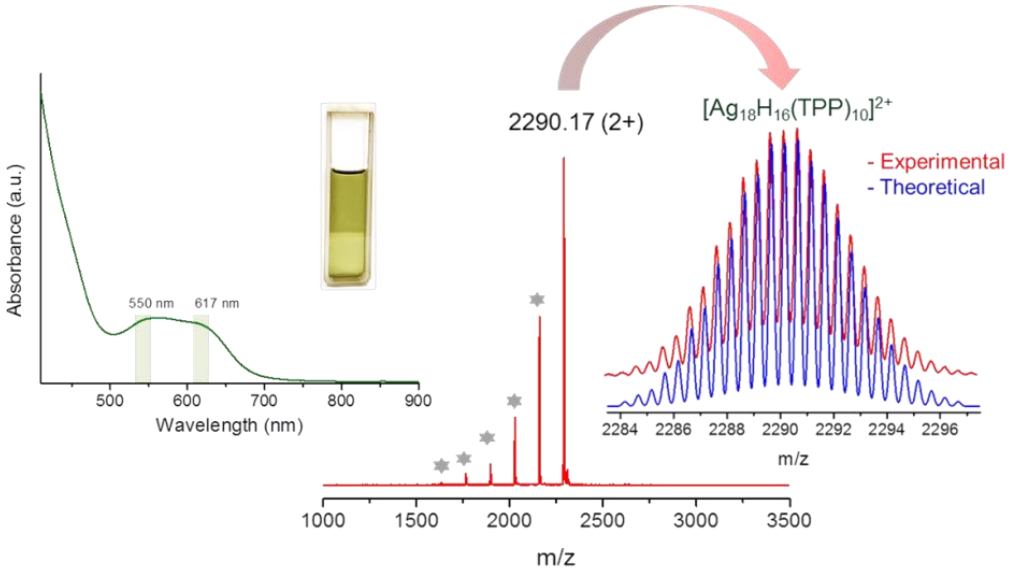

Figure S1. (Left) UV-vis absorption spectrum of Ag_{18} in methanol solution. Inset shows the photograph of the cluster. (Right) Full range ESI-MS spectrum of Ag_{18} cluster in positive ion mode. Peaks labeled * are due to the sequential losses of TPP ligands. Inset shows the exact matching of the isotopic distribution of the experimental and simulated peaks.

Synthesis of $[Ag_{24}(TPP)_{10}(HMPP)_8(TRZDT)_3]^{2+}$ NC

As shown in figure 1, Ag_{24} NC was synthesized using an adapted ligand-exchange-induced structural transformation (LEIST) method.[1] Initially, 5 mg of HMPP thiol and 3 mg of TRZDT heteroaromatic ligands were dissolved in 2 mL of methanol and rapidly added to a methanol solution of reactive hydride and phosphine protected Ag_{18} NC (15mg in 5mL) while stirring at 800 rpm. The colour immediately changed from green to purple, indicating the formation of Ag_{24} as it gradually transformed from purple to yellowish green after 3 hours of continuous reaction. The crude product was kept in methanol at 4°C for 2 days for size focusing and phase stability before being cleaned three times with water and hexane to remove inorganic salts and excess phosphine ligand. After vacuum drying, Ag_{24} was extracted by dissolving it in Methanol, dichloromethane, chloroform or dimethylformamide for further characterization.

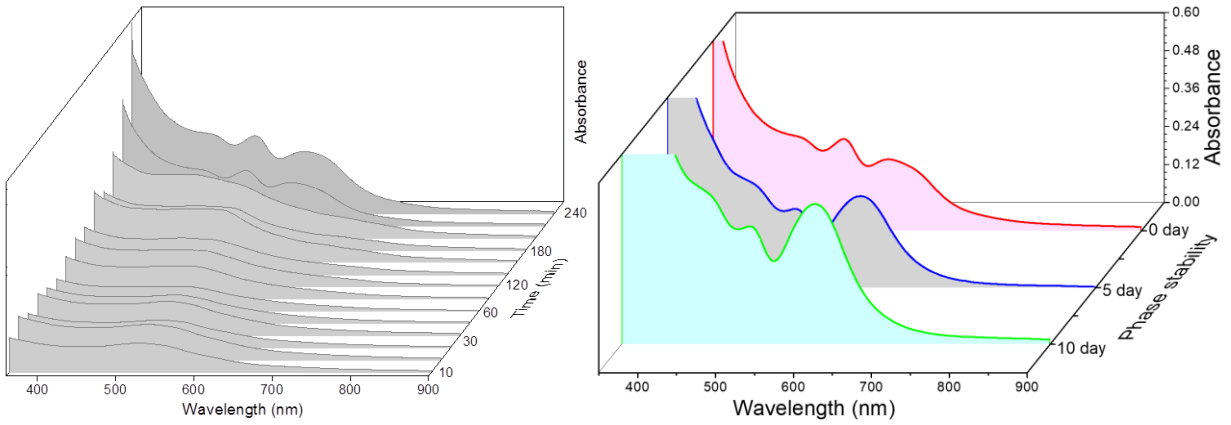

Figure S2. (Left) Time-dependent of the LEIST synthesis. (Right) Size focusing of Ag_{24} through UV-vis absorption.

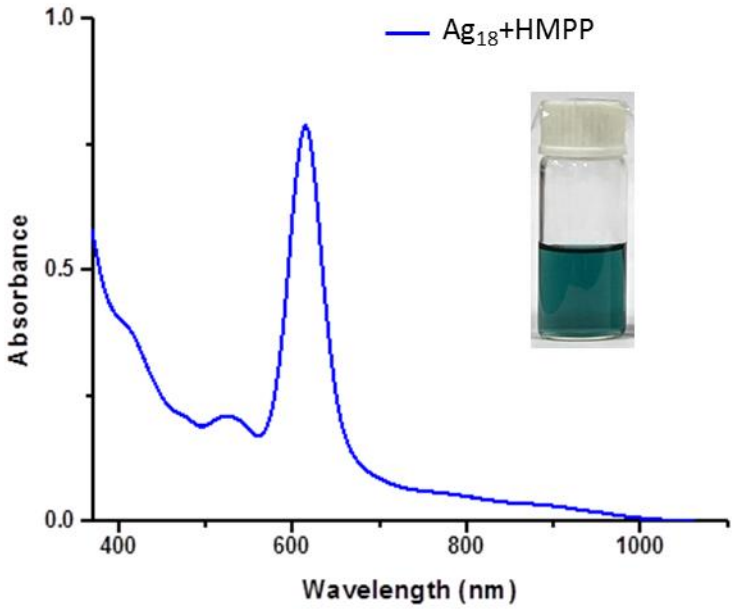

Figure S3. UV-vis absorption spectra of ligand exchange between Ag_{18} and HMPP, showing distinct color changes and spectral features indicative of the formation of clusters with different nuclearities, likely in the range $Ag_{22–24}(TPP)_{14–15}(HMPP)_{7–9}$.

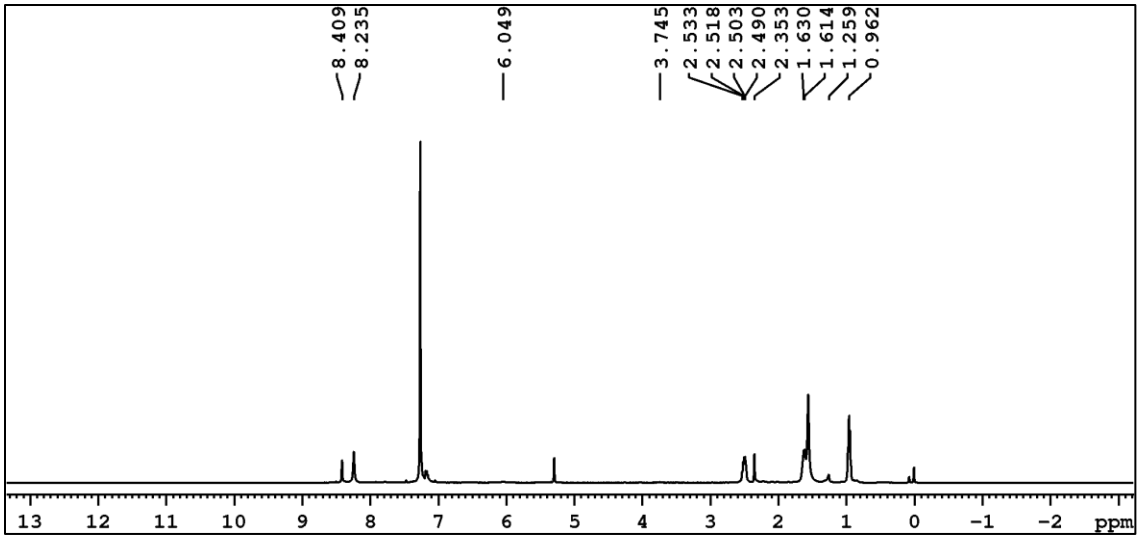

Figure S4. ^{1}H NMR spectrum (500 MHz, $CDCl_3$) of 2-mercapto-5-n-propylpyrimidine (HMMP). The terminal methyl group of the n-propyl substituent appears as a triplet at δ ~0.96 ppm (3H), while the methylene protons resonate at δ ~1.63 ppm (2H) and δ ~2. 5 ppm (2H). The pyrimidine ring proton appears as a singlet at δ ~8.2-8.4 ppm (2H). A broad resonance at δ 3.74 ppm (1H) is assigned to the thiol (S–H) proton.

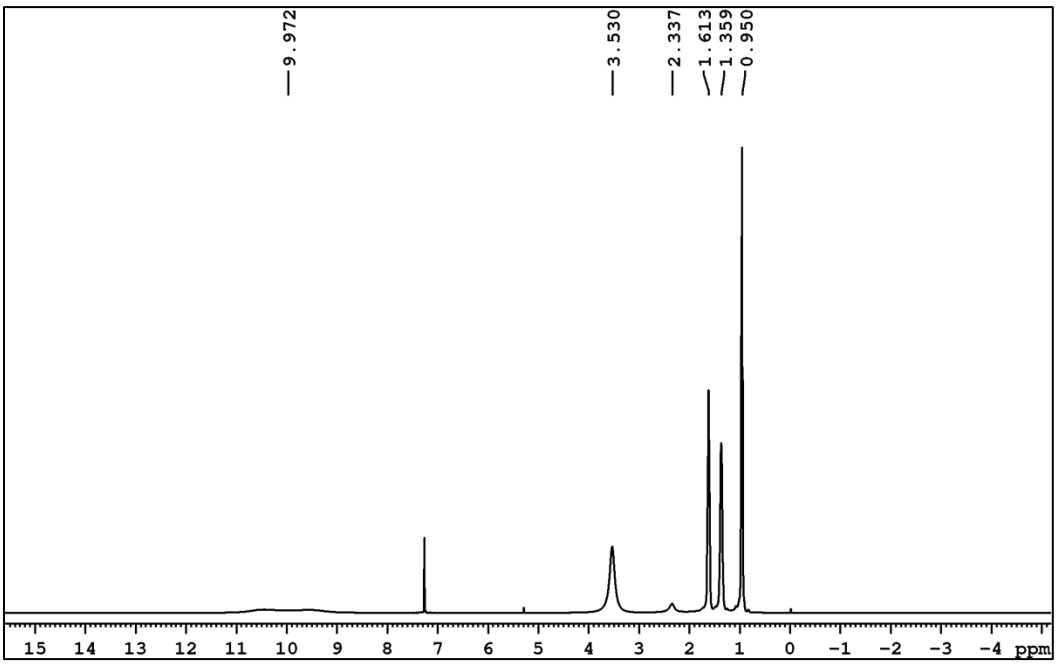

Figure S5. ^{1}H NMR spectrum (500 MHz, $CDCl_3$) of 6-(dibutylamino)-1,3,5-triazine-2,4-dithiol (TRZDT). The methylene protons directly attached to the amino nitrogen resonate at δ ~3.5 ppm (t, 4H), while the remaining butyl-chain methylene protons appear as multiplets between δ ~1.3–1.6 ppm (8H). The terminal methyl groups give a triplet at δ ~0.95 ppm (6H). The exchangeable proton(s) associated with the thiol/thione tautomeric form appear as broad resonance(s) in the downfield region. A broad resonance at δ 3.5 ppm (1H) is assigned to the thiol (S–H) proton.

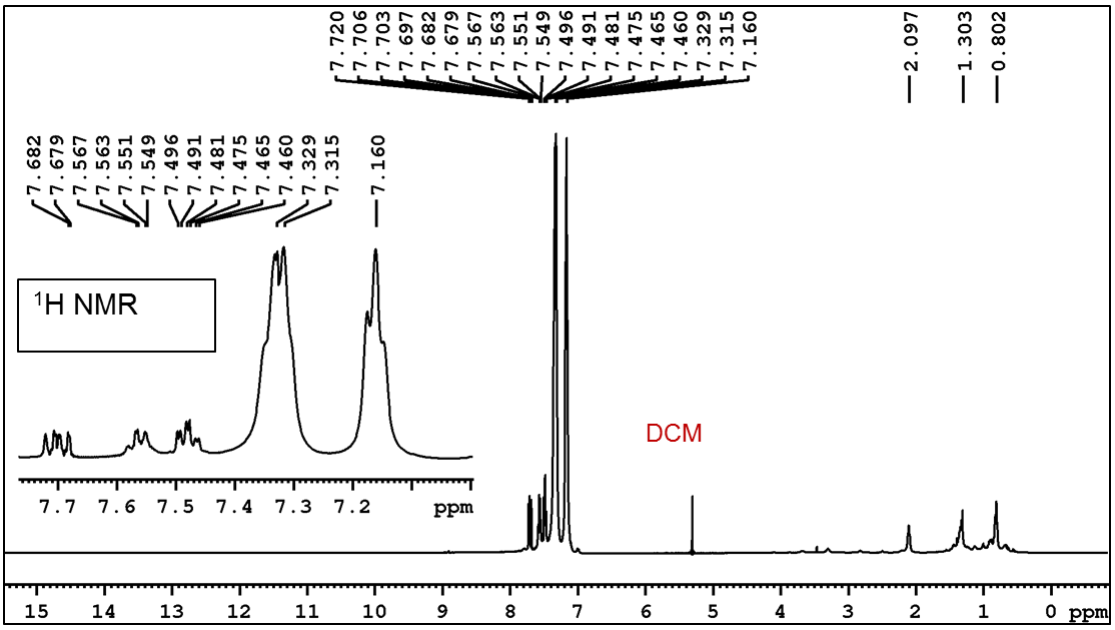

Figure S6. ^{1}H NMR of Ag_{24} NC in $CDCl_3$. The broad aromatic region between 7.1 and 7.7 ppm, arising from coordinated TPP and HMPP ligands. In addition, three well-resolved aliphatic signals at approximately 2.1, 1.3, and 0.8 ppm assigned to the propyl and butyl chains.[2,3]

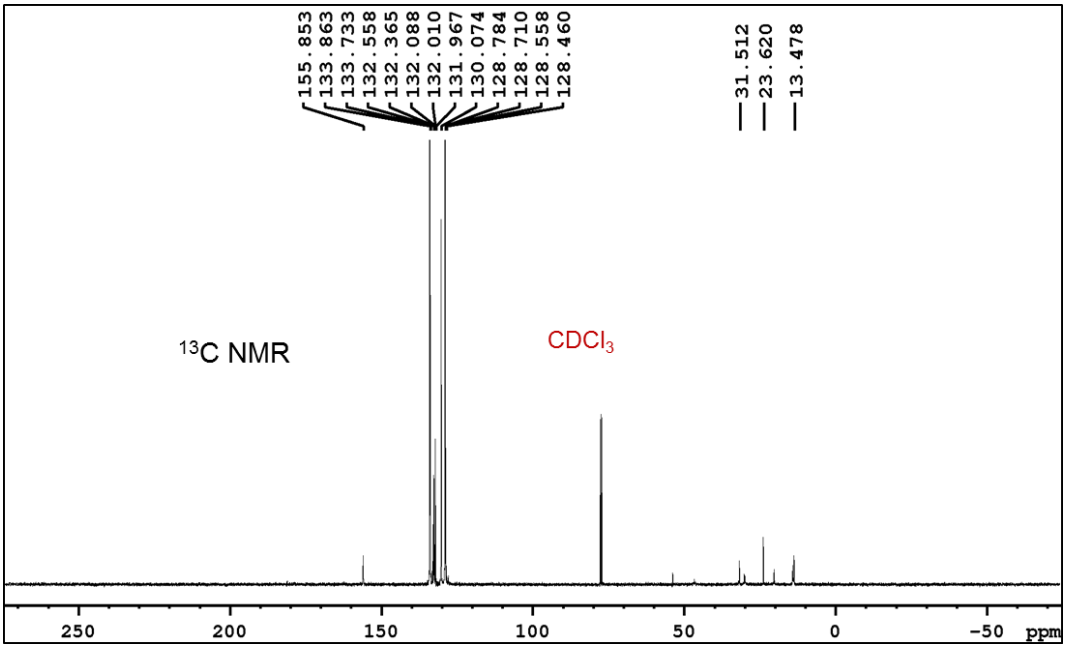

Figure S7. ^{13}C NMR of Ag_{24} NC in $CDCl_3$. The aromatic carbon resonances in the range of 128-136 ppm, together with three aliphatic signals at 31.5, 23.6, and 13.5 ppm of ligand-bound alkyl groups. [2,3]

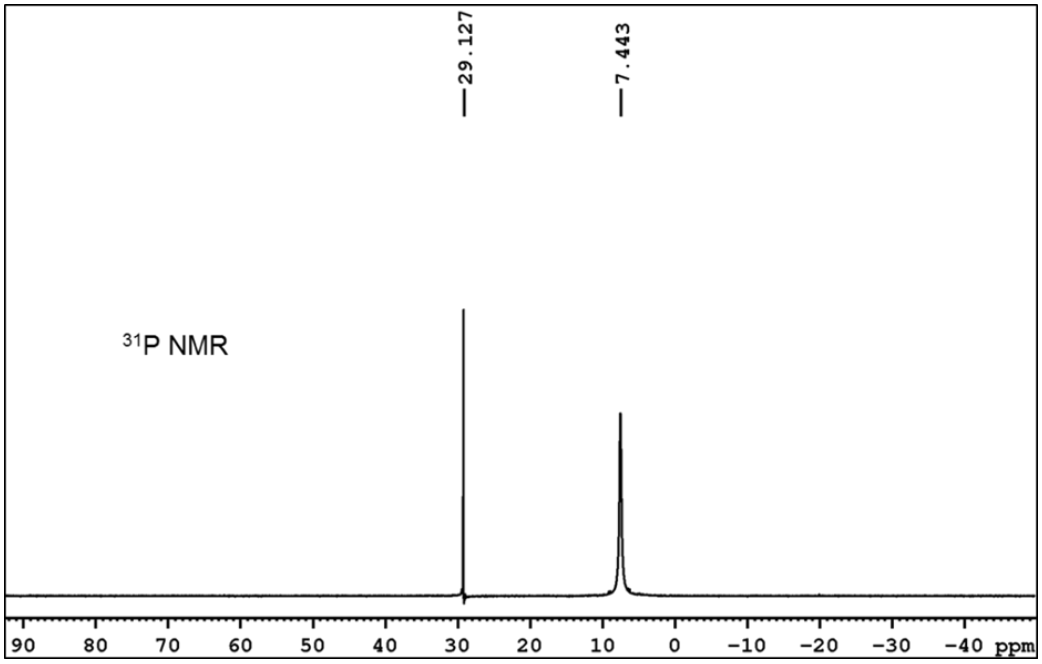

Figure S8. ^{31}P NMR of Ag_{24} NC in $CDCl_3$. The dominant resonance at 7.4 ppm, along with a signal at 29.1 ppm, indicating coordinated TPP with a small contribution from oxidized TPPO.

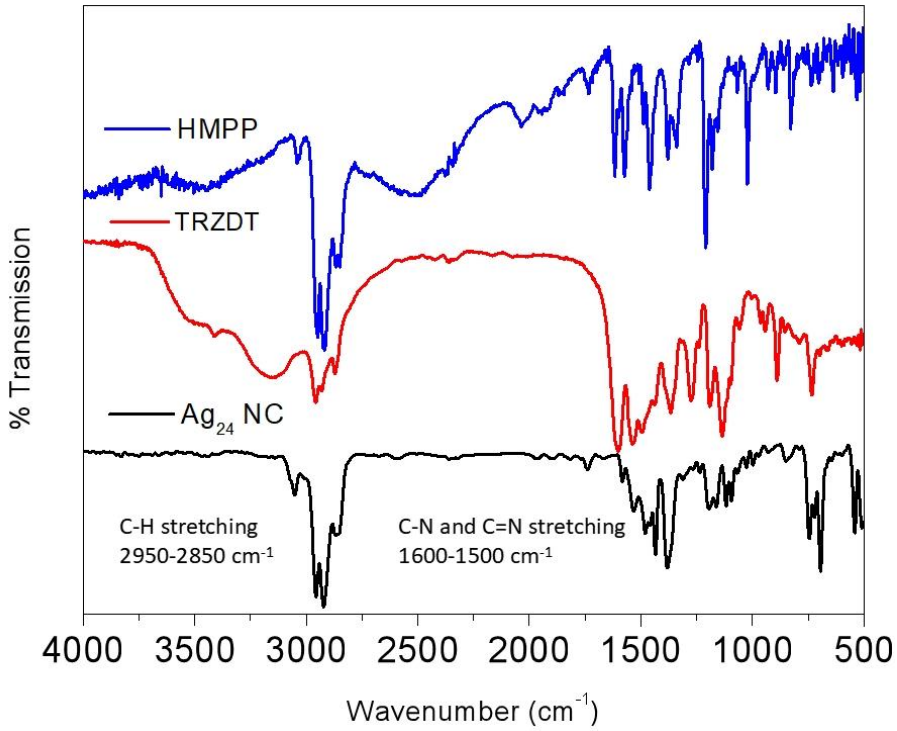

Figure S9. Comparative FT-IR-spectra of TRZDT, HMPP ligands and Ag_{24} nanocluster. The C-H stretching bands of the butyl and propyl chains are retained in the 2950-2850 cm^{-1} region, indicating that the alkyl backbones remain intact after coordination.

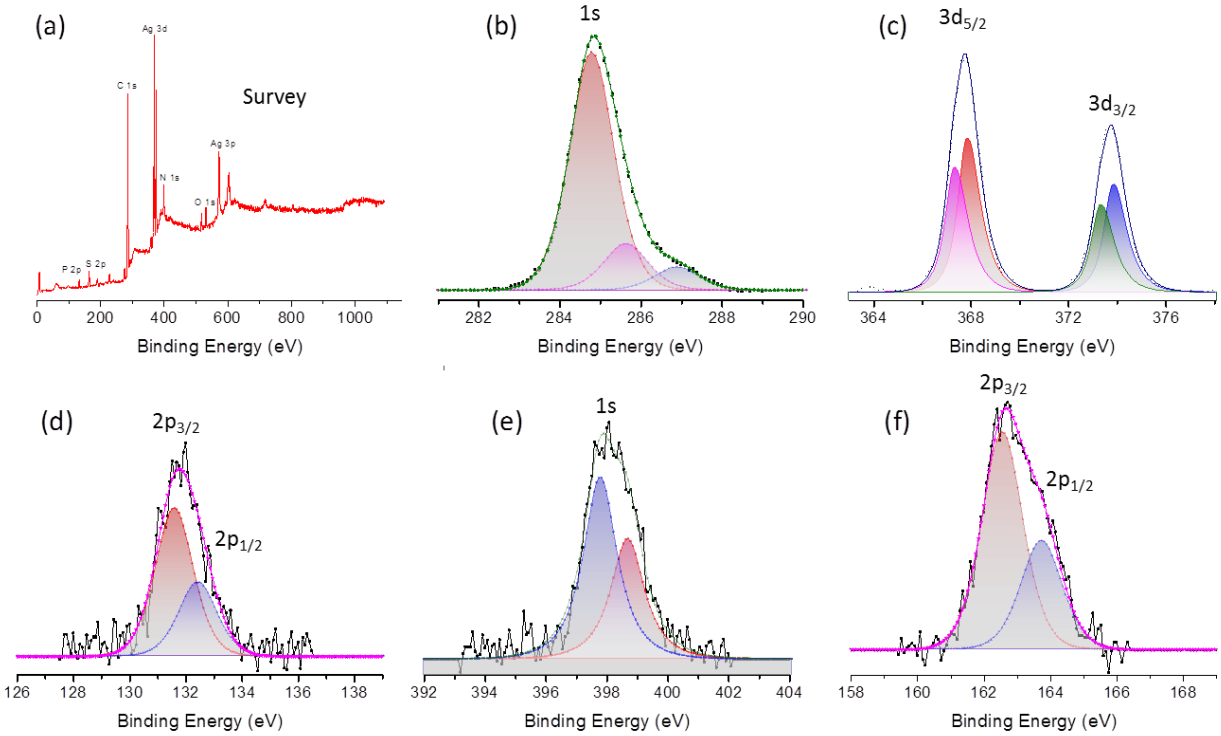

Figure S10. (a) XPS survey spectrum of Ag_{24} nanocluster showed the spectral signature of respective elements. Spectral fitting of (b) C 1s, (c) Ag 3d, (d) P 2p, (e) N 1s and (f) S 2p regions.

Table S1. XPS assignment of Ag_{24} nanocluster.

C 1s	P 2p	S 2p	Ag 3d	N 1s
284.8 – C-C Adv.	131.5 – PPh3 (MAN XPS), Phosphine complexes or M-P	162.5 – M-SR or sulphide	367.8 – Ag^0, Ag2S or sulfide	398.6 – cyanide, azide
285.6 - C-N or C-S			367.3 – Silver carbonates or fluorides or oxides (+1 state)	397.8 – cyanide, pyrimidine N
286.8 – C-N or C-S or C-Cl or Ethers or carbonyls				

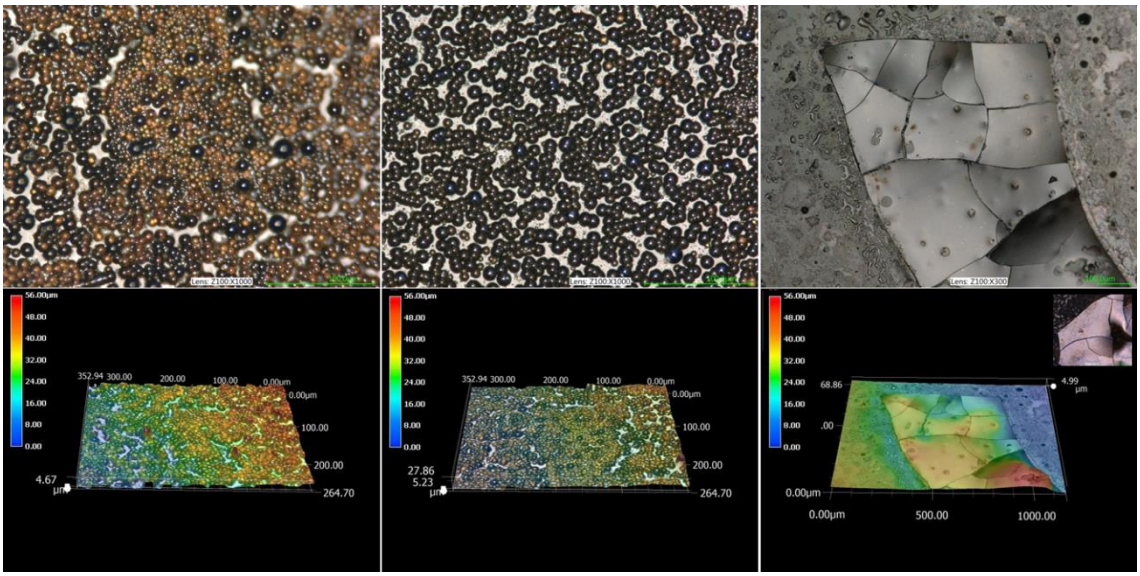

Figure S11. Optical images of Ag_{24} NC aggregates and sheets.

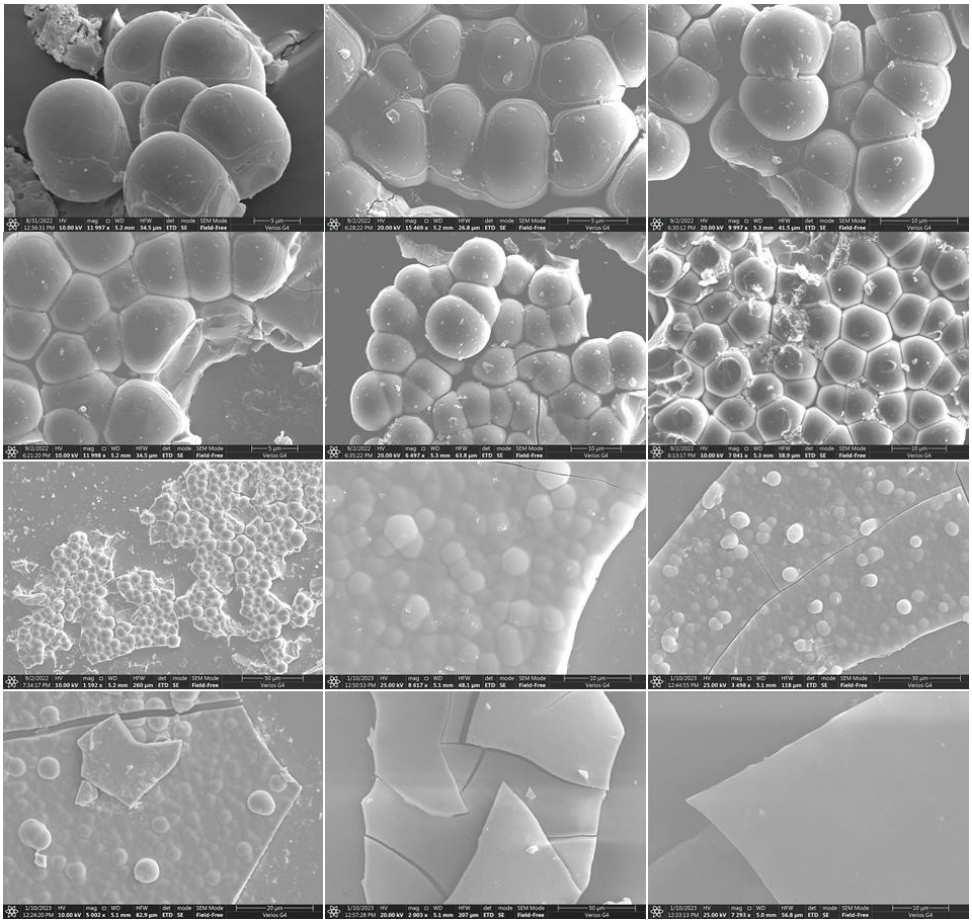

Figure S12. FESEM images of the Ag_{24} NC sheets.

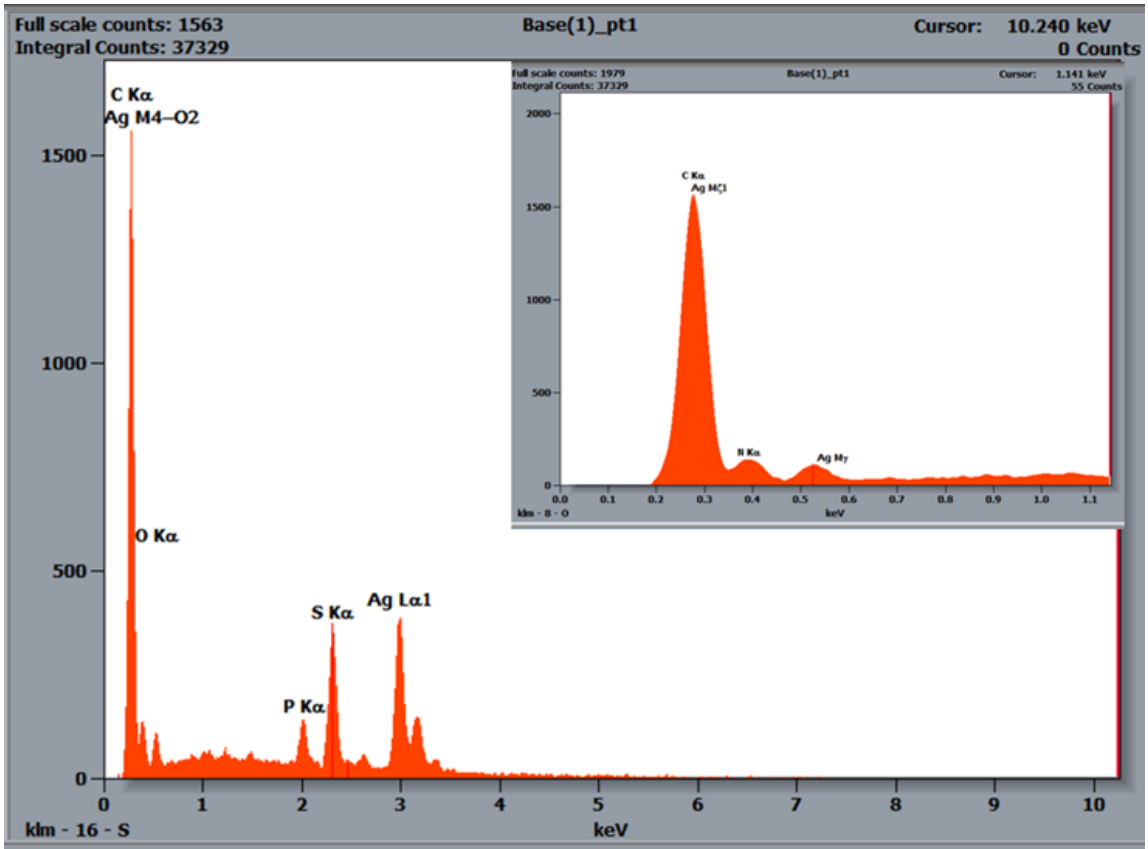

Element	Base(1)_pt1			
	Intensity	Net Counts	Weight %	Atom %
C K	0.00	9817	27.20	65.34
N K	0.00	327	3.51	7.22
P K	0.00	1196	3.05	2.84
P L	0.00	0	---	---
S K	0.00	3965	10.87	9.79
S L	0.00	0	---	---
Ag L	0.00	7203	55.38	14.82
Ag M	0.00	77	---	---
			100.00	100.00

Figure S13. FESEM-EDX analysis with elemental compositions (C, N, P, S, and Ag) consistent with the proposed Ag_{24} formulation, confirming retention of the cluster composition in the assembled state.

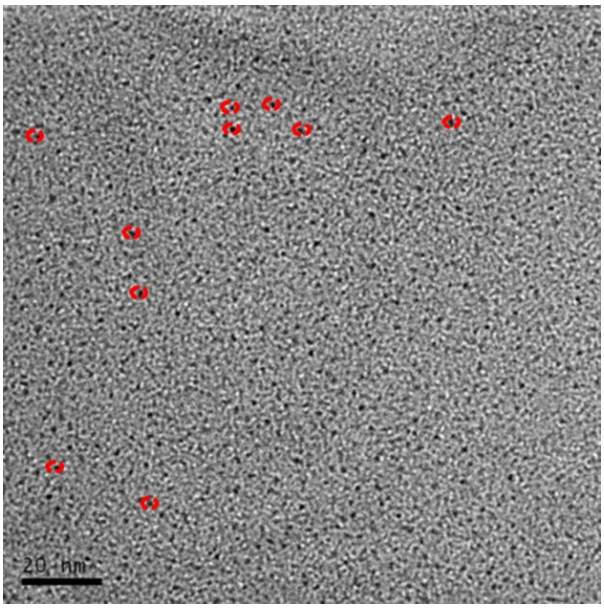

Figure S14. HR-TEM images of Ag_{24} NC shows a uniform particle size below 2 nm, consistent with atomically precise Ag_{24} cluster core size.

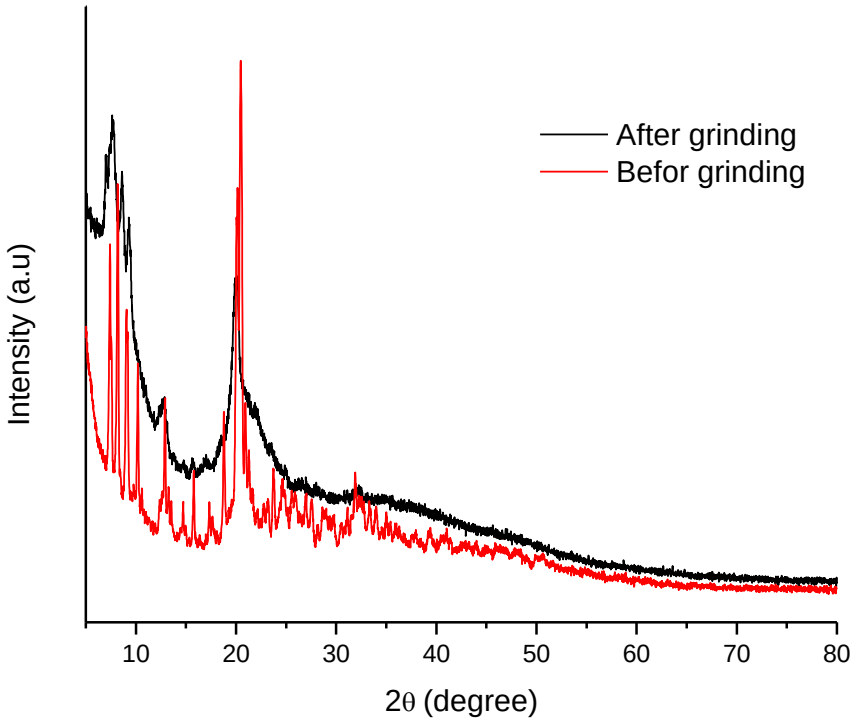

Figure S15. Powder X-ray diffraction (PXRD) patterns of Ag_{24} aggregate sheets before and after mechanical grinding. The ground sample retains the characteristic diffraction peaks of the pristine material, indicating preservation of the crystalline phase. Minor variations in peak intensity and broadening are attributed to grinding-induced reduction in crystallite size and increased structural disorder.

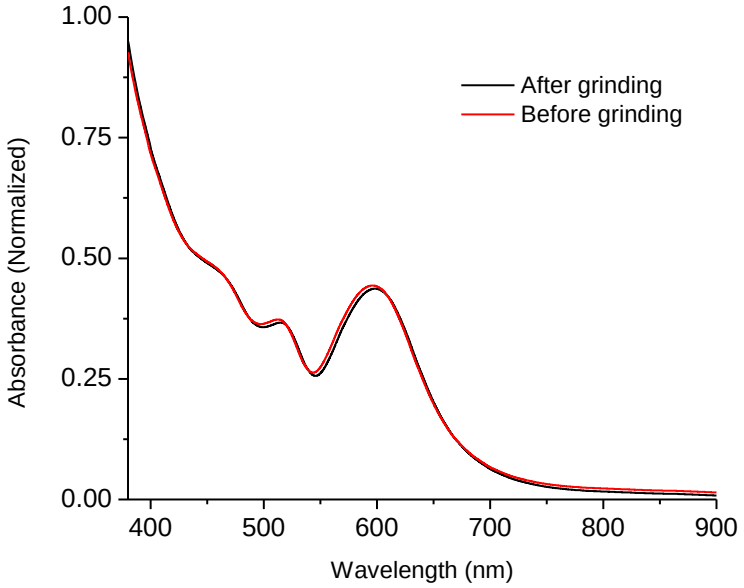

Figure S16. UV–Vis absorption spectra of Ag_{24} NC before and after grinding, recorded in methanol. The nearly identical absorption profiles indicate that the Ag_{24} cluster core remains intact after grinding.

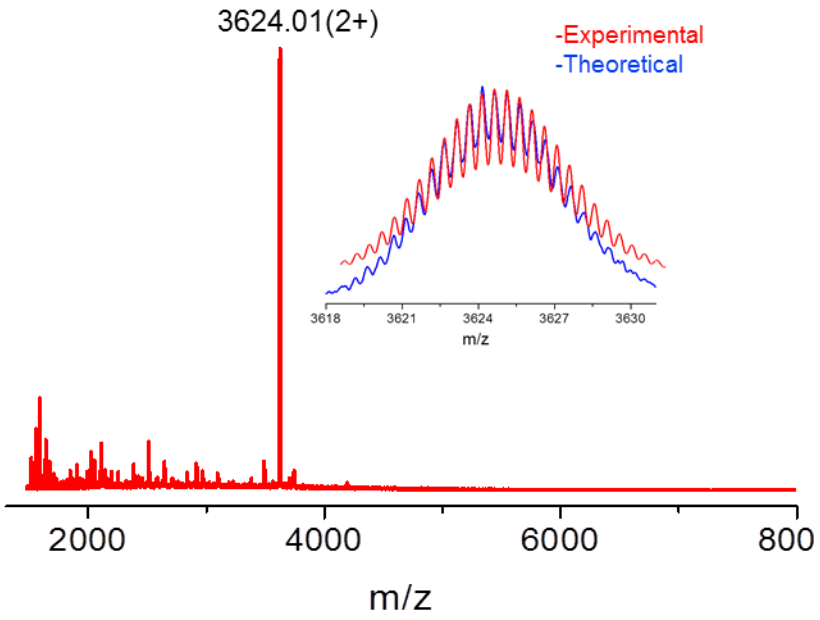

Figure S17. The ESI mass spectrum of the ground sample exhibits the same doubly charged molecular ion peak as the pristine material (m/z 3623.99 before grinding; m/z 3624.01 after grinding), indicating retention of the molecular composition of the Ag24 cluster during the grinding process**.**

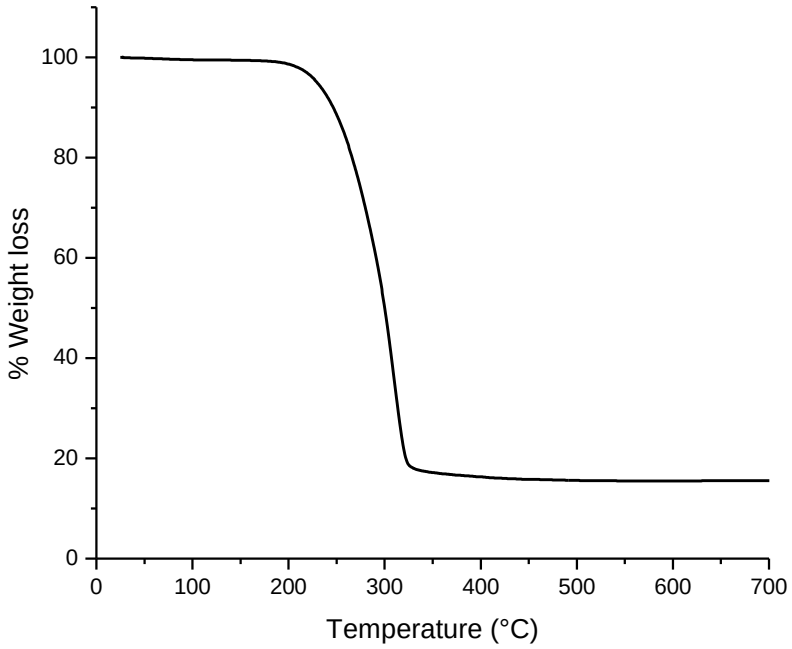

Figure S18. Thermogravimetric analysis (TGA) of Ag_{24}, showing thermal stability up to 180 °C, with the maximum mass loss observed at 360 °C.

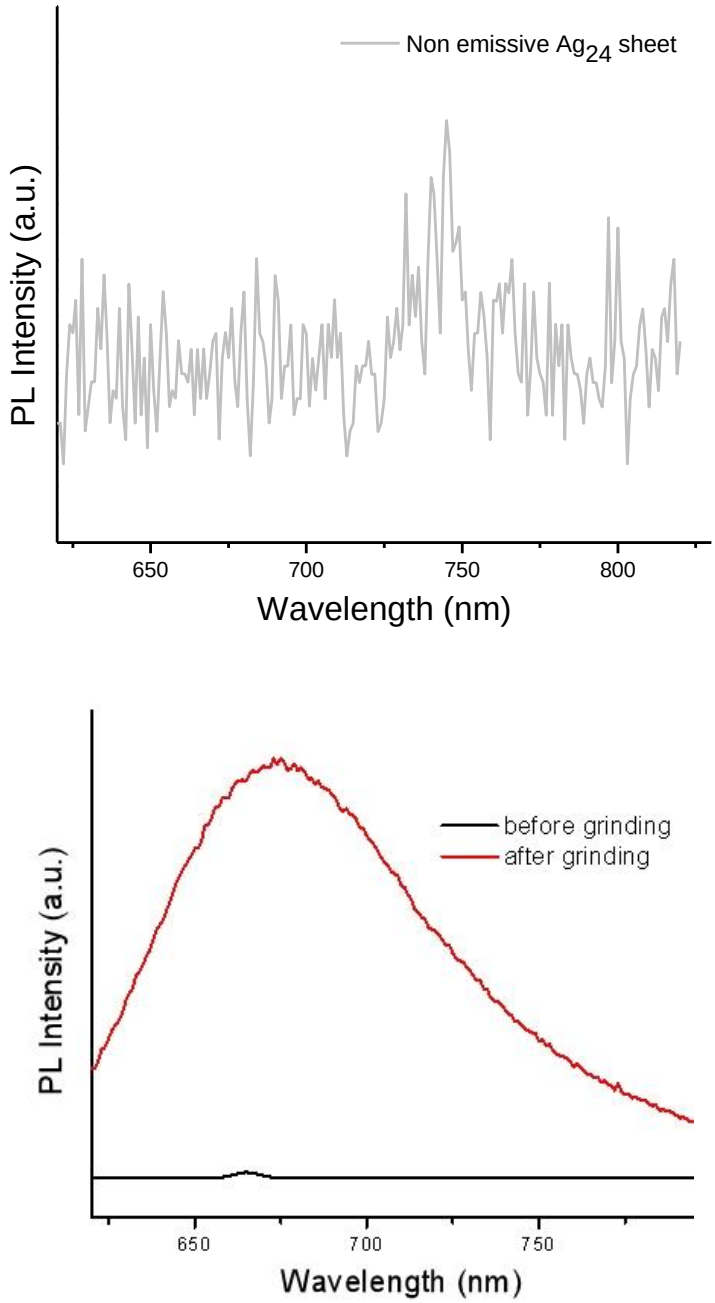

Figure S19. The Ag_{24} nanocluster shows aggregation-induced quenching upon self-assembly into non-emissive sheets (top), while emission reappears after grinding (bottom), demonstrating mechanoluminescence.

References:

1 Bootharaju, M. S.; Dey, R.; Gevers, L. E.; Hedhili, M. N.; Basset, J.-M.; Bakr, O. M. A New Class of Atomically Precise, Hydride-Rich Silver Nanoclusters Co-Protected by Phosphines. *J. Am. Chem. Soc.* **2016**, *138* (42), 13770–13773. https://doi.org/10.1021/jacs.6b05482.

2 Nguyen, T.-A. D.; Cook, A. W.; Wu, G.; Hayton, T. W**.** Subnanometer-Sized Copper Clusters: A Critical Re-evaluation of the Synthesis and Characterization of $Cu_8(MPP)_4$ (HMPP = 2-Mercapto-5-*n*-propylpyrimidine). *Inorg. Chem.* **2017**, *56* (14), 8390–8396. https://doi.org/10.1021/acs.inorgchem.7b01062.

3 Jana, A.; Dar, W. A.; Jana, S. K.; Poonia, A. K.; Yadav, V.; Roy, J.; Chandra, S.; Adarsh, K. N. V. D.; Ras, R. H. A.; Pradeep, T. Photoconversion of Ag_{31} to Ag_{42} Initiated by Solvated Electrons. *Chem. Mater*. **2023**, *35* (17), 7020–7031. https://doi.org/10.1021/acs.chemmater.3c01293.

---End---